

PAPER • OPEN ACCESS

Effect of SnO₂ substitution on microwave dielectric characteristics of Zn_{0.15}Nb_{0.3}Ti_{0.55}O₂ ceramics

To cite this article: H C Yang *et al* 2019 *IOP Conf. Ser.: Mater. Sci. Eng.* **479** 012032

View the [article online](#) for updates and enhancements.



IOP | ebooks™

Bringing you innovative digital publishing with leading voices to create your essential collection of books in STEM research.

Start exploring the collection - download the first chapter of every title for free.

Effect of SnO₂ substitution on microwave dielectric characteristics of Zn_{0.15}Nb_{0.3}Ti_{0.55}O₂ ceramics

H C Yang^{1,2}, S R Zhang^{1,2,4}, Y W Chen^{1,2}, H Y Yang^{1,2}, Y Yuan^{1,2,3} and E Z Li^{1,2}

¹National Engineering Research Center of Electromagnetic Radiation Control Materials, University of Electronic Science and Technology of China, Chengdu, 610054;

²Key Laboratory of Multi-Spectral Absorbing Materials and Structures of Ministry of Education, University of Electronic Science and Technology of China, Chengdu, 610054;

³Institute of Electronic and Information Engineering of UESTC in Guangdong Dongguan 523808, People's Republic of China

⁴E-mail: zsr@uestc.edu.cn

Abstract. The relevance of Sn⁴⁺ substituted for Ti⁴⁺ of Zn_{0.15}Nb_{0.3}Ti_{0.55}O₂ ceramics is investigated. X-ray diffraction patterns indicate that the major phase can be matched with Zn_{0.15}Nb_{0.3}Ti_{0.55}O₂ and a second phase ZnTiNb₂O₈ appears in different composition. The content of ZnTiNb₂O₈ phase gradually increases along with more substitution, which is contributed to the decline of ϵ_r . The decrease of grain size and the observed pores have negative influence on $Q \times f$ values. And the τ_f values move towards a lower value, corresponding to the variation of ϵ_r . An optimal combination of microwave dielectric properties is: $\epsilon_r=83.2$, $Q \times f=15456$ GHz, $\tau_f=301.5$ ppm/°C with $x=0.03$, sintered at 1050 °C.

1. Introduction

Microwave dielectric ceramic is core component of microwave devices in wireless communication area over decades. After the initial report about dielectric properties of BaO-TiO₂ binary system by H. M. O'Bryan in 1974 [1], researchers continuously explore new ceramics with different permittivity and satisfied quality factor.

Compared with the typical high dielectric constant perovskites (ABO₃) ceramics, ZnO-Nb₂O₅-TiO₂ system is a new family with adjustable permittivity and lower sintering temperature [2, 3]. For Zn₃Nb₂O₈ phase with an order super-structure of α -PbO₂, it was demonstrated to be promising materials with excellent properties: $\epsilon_r=21.2$, $Q \times f=79200$ GHz, $\tau_f=-73$ ppm/°C [4]. And the columbite ZnNb₂O₆ has been concentrated investigated due to its high $Q \times f$ value approach to 83700 GHz [5]. Besides, the temperature coefficient of both Zn₃Nb₂O₈ and ZnNb₂O₆ can be tunable to near zero by adding TiO₂ [6,7]. More recently, the investigations about the structure-properties relationship of ZnTiNb₂O₈ ceramics are reports systematically [8], *i.e.* ZnTi(Nb_{1-x}Ta_x)₂O₈ [9], Mg_{0.5}Zn_{0.5}TiNb₂O₈ [10], (Zn_{1-x}Co_x)TiNb₂O₈ [11], Zn(Ti_{1-x}Sn_x)Nb₂O₈ [12] and so on. Furthermore, Zn_{0.15}Nb_{0.3}Ti_{0.55}O₂ in rutile structure was reported in (Zn_{1/3}B_{2/3}⁵⁺)_xTi_{1-x}O₂ (B⁵⁺=Nb, Ta) ceramics when $x=0.45$ [13]. And then, it is a second phase when Ca²⁺ and Sn⁴⁺ co-substituted in ZnTiNb₂O₁₀ [14]. Zn_{0.15}Nb_{0.3}Ti_{0.55}O₂ also appeared when Co²⁺ occupied in Zn-site [11], Sb⁵⁺ substituted for Nb-site [15] and Co together with Ta co-doped in Zn_{0.5}Ti_{0.5}NbO₄ [16], in which favourable effect on the microwave dielectric properties



was verified: $\epsilon_r=35.93$, $Q \times f=35125$ GHz, $\tau_f=0$ ppm/ $^{\circ}$ C; $\epsilon_r=33.84$, $Q \times f=31000$ GHz, $\tau_f=-67.91$ ppm/ $^{\circ}$ C and $\epsilon_r=38.02$, $Q \times f=23550$ GHz, $\tau_f=4.62$ ppm/ $^{\circ}$ C, respectively. Meanwhile, Li et al demonstrated that $\text{Li}_2\text{O}-\text{B}_2\text{O}_3-\text{SiO}_2$ glass can enhance the sintering process of $\text{Zn}_{0.15}\text{Nb}_{0.3}\text{Ti}_{0.55}\text{O}_2$ [17] and $\text{ZnO}-\text{B}_2\text{O}_3-\text{SiO}_2$ glass was a satisfied sintering aid for $\text{Zn}_{0.9}\text{Mg}_{0.1}\text{TiO}_3-\text{Zn}_{0.15}\text{Nb}_{0.3}\text{Ti}_{0.55}\text{O}_2$ ceramics [18]. Besides, x $\text{Zn}_{0.5}\text{Ti}_{0.5}\text{NbO}_4-(1-x)$ $\text{Zn}_{0.15}\text{Nb}_{0.3}\text{Ti}_{0.55}\text{O}_2$ ceramics possessed a near zero temperature coefficient when $x=0.516$ [19]. However, the research about structure modification for $\text{Zn}_{0.15}\text{Nb}_{0.3}\text{Ti}_{0.55}\text{O}_2$ ceramics by ions substitution and the dependence of phase composition upon microwave dielectric properties has been hardly reported.

Indeed, it is verified that the replacement of Sn for Ti could optimize the microwave dielectric properties of Sr_2TiO_4 [20], and it crystalized in a structure of tetragonal phase (I4/mmm) firstly and then transform into orthorhombic type (Pccn). Adding SnO_2 into initial composition of BaTi_4O_9 [21], the dielectric constant linearly decreased from 38.9 to 37.5, $Q \times f$ values distinctly changed from 45600 to 33100 GHz, and τ_f values shifted in a narrow region. Specially, Sn^{4+} has a limited solid solubility around $x=0.15$ in $\text{Zn}(\text{Ti}_{1-x}\text{Sn}_x)\text{Nb}_2\text{O}_8$ [12]. Although secondary phase of BaSm_2O_4 and $\text{Sn}_2(\text{Sn,Ti})_2\text{O}_7$ were observed in the co-substituted $\text{Ba}_{6-3x}(\text{Sm}_{1-y}\text{Nd}_y)_{8+2x}(\text{Ti}_{1-z}\text{Sn}_z)_{18}\text{O}_{54}$ ceramics, excellent microwave dielectric characteristics were achieved with $y=0.8$ and $z=0.05$ [22]. Specially, Sn^{4+} has been applied to $\text{ZnO}-\text{Nb}_2\text{O}_5-\text{TiO}_2$ system by Li et al [23] and Wang et al [24] to modify the microwave dielectric properties.

Hence, referring to the rare reports of $\text{Zn}_{0.15}\text{Nb}_{0.3}\text{Ti}_{0.55}\text{O}_2$ -based ceramics, the approximate radii of Sn^{4+} and Ti^{4+} as well as the positive impact of substitution Sn for Ti on microwave dielectric properties in parallel investigations, the introduction of SnO_2 into $\text{Zn}_{0.15}\text{Nb}_{0.3}\text{Ti}_{0.55}\text{O}_2$ may generate improvement of dielectric characteristics integrally. In this work, the effect of phase composition on the evolution of microstructure, density and microwave dielectric properties was investigated in detail after doping SnO_2 in $\text{Zn}_{0.15}\text{Nb}_{0.3}\text{Ti}_{0.55}\text{O}_2$ ceramics.

2. Experimental methods

ZnO , Nb_2O_5 , TiO_2 and SnO_2 powders with a reagent-grade were used to prepare $\text{Zn}_{0.15}\text{Nb}_{0.3}\text{Ti}_{0.55-x}\text{Sn}_x\text{O}_2$ ($x=0\sim 0.05$) ceramics via solid state method. All the oxide powders were weighed and then mixed for 6 h, where zirconia balls and deionized water were medium. After putting into the drying oven, the powders were calcined at 950 $^{\circ}$ C for 4 h. Subsequently, the calcined compositions were milled again to obtain more uniform powder. Adding 3 wt. % PVA into the dried powers, the mixture was pressed into disks ($\Phi 15\text{mm} \times 7\text{mm}$). The formed cylindrical samples were sintered in the temperature range of 1025 $^{\circ}$ C ~ 1075 $^{\circ}$ C for 4 h to measure relevant properties.

The X-ray diffraction patterns (Philips X'Pert ProMPD, Amsterdam, The Netherlands) were obtained in the region of $10^{\circ} \sim 120^{\circ}$ with a minimal step of 0.013° using Cu $K\alpha$ radiation. The micrographic images of the ceramics with highest density were recorded through scanning electron microscopy (SEM, FEI Inspect F, the United Kingdom). Hakki-Coleman dielectric resonator method was a widespread tool to collect the microwave dielectric properties equipped with a network analyzer (HP83752A, the United States) in TE011 mode. The τ_f values was calculated according to the measured resonant frequency at 25 $^{\circ}$ C and 85 $^{\circ}$ C as follow:

$$\tau_f = \frac{f_{85} - f_{25}}{f_{25} \times (85 - 25)} \quad (1)$$

Where f_{85} and f_{25} represent the resonant frequencies at temperature 85 $^{\circ}$ C and 25 $^{\circ}$ C in the TE011 mode, respectively.

3. Results and discussion

3.1. Crystal structure analysis

The stacked XRD patterns of $\text{Zn}_{0.15}\text{Nb}_{0.3}\text{Ti}_{0.55}\text{O}_2$ -based well sintered ceramics are displayed in Figure 1 (a), and the enlarged patterns with 2θ ranging from $25^{\circ}\sim 32^{\circ}$ are presented in Figure 1 (b). The

reflection peaks of different composition can be allocated to $\text{Zn}_{0.15}\text{Nb}_{0.3}\text{Ti}_{0.55}\text{O}_2$ (JCPDS #79-1186) and $\text{ZnTiNb}_2\text{O}_8$ (JCPDS #88-1973), corresponding to a space group P42/mmm (136) and Pbcn (60), respectively. As shown, along with the increasing addition of SnO_2 , the strongest peak of $\text{ZnTiNb}_2\text{O}_8$ which is indexed as the crystallographic plane (111) become more and more apparent. It is indicating that the content of orthorhombic $\text{ZnTiNb}_2\text{O}_8$ phase continuously goes up.

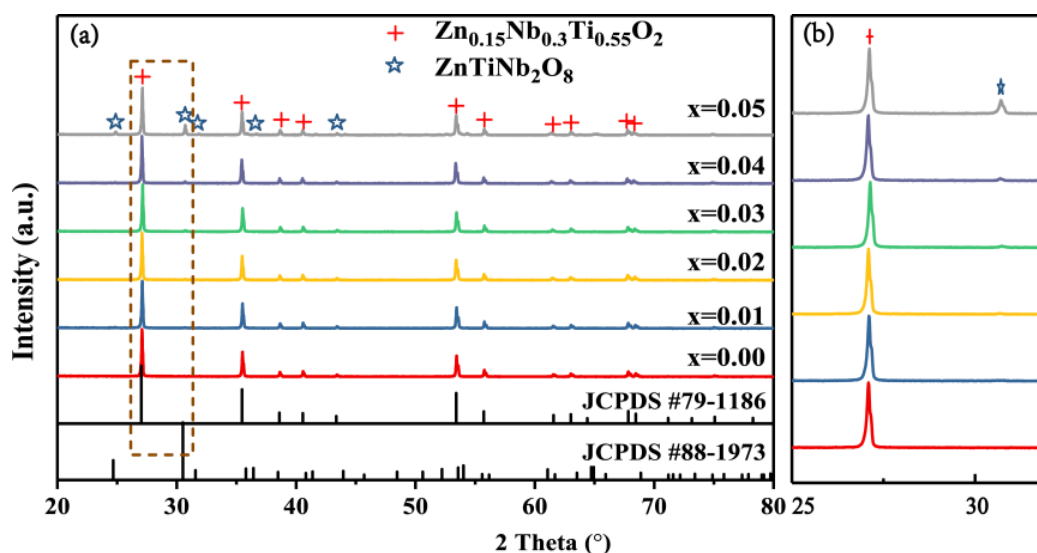


Figure 1. (a) The XRD patterns of different $\text{Zn}_{0.15}\text{Nb}_{0.3}\text{Ti}_{0.55}\text{O}_2$ -based ceramics; (b) The enlarged XRD patterns of $2\theta=25\sim 32^\circ$.

The crystal structure of the $\text{Zn}_{0.15}\text{Nb}_{0.3}\text{Ti}_{0.55}\text{O}_2$ and $\text{ZnTiNb}_2\text{O}_8$ phase are plotted in Figure 2 (a) and (b). Since $\text{Zn}_{0.15}\text{Nb}_{0.3}\text{Ti}_{0.55}\text{O}_2$ and TiO_2 both crystallized in a rutile type, Zn^{2+} , Ti^{4+} couple with Nb^{5+} occupy the center of octahedron, named a Wyckoff position of 2a, while all the oxygen atoms distribute in 4f Wyckoff position. For $\text{ZnTiNb}_2\text{O}_8$ phase, three kinds of cations stay the same 4c Wyckoff position, and O scatters in the 8d Wyckoff position. The polyhedron connects with each other through the sharing-edge and the apical oxygen in the two phases.

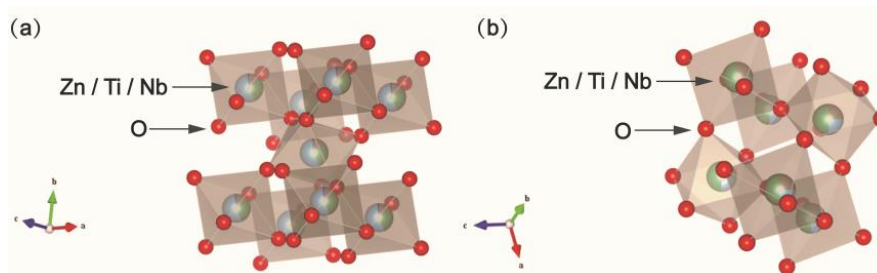


Figure 2. The structure of $\text{Zn}_{0.15}\text{Nb}_{0.3}\text{Ti}_{0.55}\text{O}_2$ (a) and $\text{ZnTiNb}_2\text{O}_8$ (b).

3.2. Surface microstructure and density analysis

The surface micrographs of doped $\text{Zn}_{0.15}\text{Nb}_{0.3}\text{Ti}_{0.55}\text{O}_2$ -based ceramics sintered at 1050°C are given in Figure 3 (a: $x=0$; b: $x=0.03$; c: $x=0.04$). The whole images exhibit obvious grain boundary and compact microstructure except $x=0.04$ with some pores. Due to the small amount of the $\text{ZnTiNb}_2\text{O}_8$ phase, the shape of the grains nearly maintains the same in the observed area. It is clear that the grain size goes through a distinct variation. According to Q. J. Mei et al, the grain is extremely small of $\text{ZnTiNb}_2\text{O}_8$ ceramics [25]. Therefore, with more content of the second phase, the grain size inevitably declines. Subsequently, the small grain will lead to more grain boundary and more pores as we can detect in the photos, which would have a negative influence on the microwave dielectric properties.

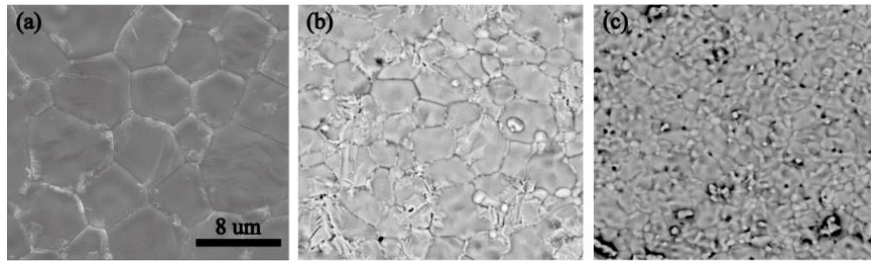


Figure 3. The microstructure of $\text{Zn}_{0.15}\text{Nb}_{0.3}\text{Ti}_{0.55}\text{O}_2$ -based ceramics (a) $x=0$; (b) $x=0.03$; (c) $x=0.04$.

3.3. Microwave dielectric properties:

A persistent decline of dielectric constant is plotted in Figure 4 (a), and the values of different sintering temperature are displayed in different color. As shown, dielectric constant values sintered at 1050°C are integrally higher than the corresponding values of other temperature, indicating that the ceramics are more compact sintered at 1050°C . Meanwhile, the decrement of the permittivity ranging from 92.03 to 72.72 is ascribed to the appearance of $\text{ZnTiNb}_2\text{O}_8$ phase. Generally, the dielectric constant of composite ceramics can be predicted by Logarithmic mixing rule:

$$\ln \varepsilon_r = V_1 \ln \varepsilon_1 + V_2 \ln \varepsilon_2 \quad (2)$$

Where the relevant values are selected from the peer's work, for $\text{Zn}_{0.15}\text{Nb}_{0.3}\text{Ti}_{0.55}\text{O}_2$, the $\varepsilon_1=93.58$, for $\text{ZnTiNb}_2\text{O}_8$, the $\varepsilon_2=34.3$, and V_i means the volume fraction of each phase. According to the formula, the ε_r of the multiphase ceramics should be linearly dropped with the increasing content of low permittivity phase. Therefore, the variation of the measured values is reasonable. On the other hand, permittivity is closely related to relative density of the ceramics. Figure 4 (b) shows the relative densities of the samples sintered in different conditions. For different composition, the ceramics sintered at 1050°C all reach to the highest density, corresponding to the relatively larger ε_r . And the change tendency of the relative density is similar to the variation of ε_r .

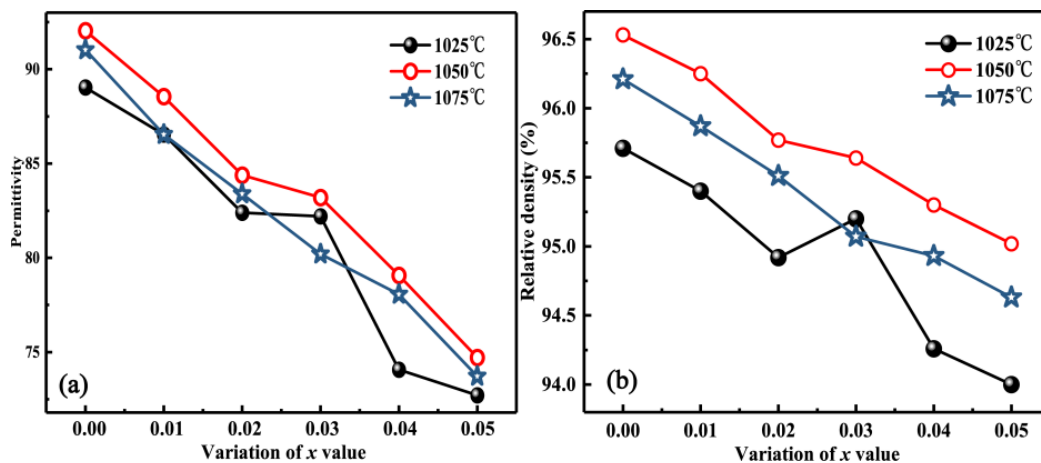


Figure 4. Variation of permittivity (a) and relative density (b) of $\text{Zn}_{0.15}\text{Nb}_{0.3}\text{Ti}_{0.55}\text{O}_2$ -based ceramics sintered at different temperature.

Figure 5 presents the fluctuation of the experimental $Q \times f$ values. The values of samples with the highest density increase to 15456 GHz at $x = 0.03$ following a slowly decline to 12791 GHz. As known, the factors that affect the dielectric loss are usually concluded to intrinsic and extrinsic parts. Combining with the analysis above, a second phase is confirmed by XRD and the obvious change of grain size is observed *via* SEM. The augment of the $Q \times f$ values stems from the growth of grains and a more uniform microstructure. Besides, the composition of ceramic will affect the $Q \times f$ values chiefly.

The lower dielectric loss of $\text{ZnTiNb}_2\text{O}_8$ leads to a more excellent $Q \times f$ values. Nevertheless, the effect of grain boundary is more apparent than the influence of phase content of $\text{ZnTiNb}_2\text{O}_8$ because a lot of small grains appear when $x \geq 0.04$. Up to our knowledge, more grain boundary generated more dielectric loss, and the clear pores with $x=0.04$ both have negative impact on $Q \times f$ values.

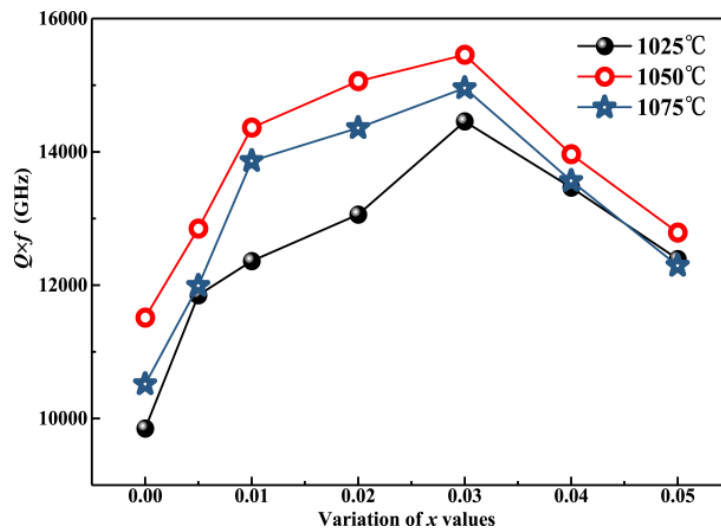


Figure 5. Variation of $Q \times f$ values of $\text{Zn}_{0.15}\text{Nb}_{0.3}\text{Ti}_{0.55}\text{O}_2$ -based ceramics sintered at different temperature.

Temperature coefficient of resonant frequency τ_f reflects the stability of crystal structure. An approximate zero τ_f value corresponds to a more stable system. In our work, the τ_f values vary in an extensive region, decreasing from 346.00 to 257.67 ppm/°C. The prior reports illustrate that the variation of τ_f values is associated with τ_ε :

$$\tau_f = -(\tau_\varepsilon + \frac{\alpha_l}{2}) \quad (3)$$

Where the τ_ε is reckon as a parameter determined by polarizability and it would go up as the drop of ε_r values. As for α_l , it is a stable values changing in a narrow range in microwave dielectric ceramics. According to the results in Figure 6, the τ_f values and ε_r values of the ceramics sintered at 1050°C both linearly declined, suggesting a more stable materials are obtained with increasing x value.

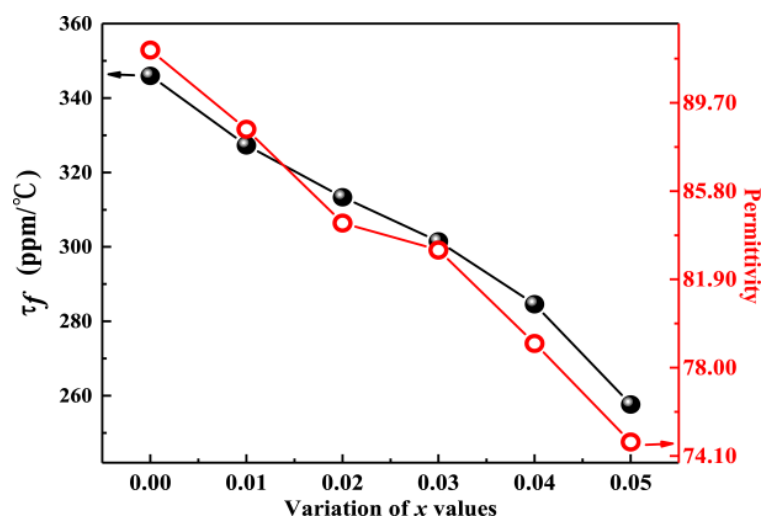


Figure 6. Variation of τ_f and ε_r values of $\text{Zn}_{0.15}\text{Nb}_{0.3}\text{Ti}_{0.55}\text{O}_2$ -based ceramics sintered at 1050 °C.

4. Conclusions

Multiphase compact $Zn_{0.15}Nb_{0.3}Ti_{0.55}O_2$ -based ceramics have been prepared in this investigation. The most satisfied microwave dielectric property is described as: $\epsilon_r=83.2$, $Q \times f=15456$ GHz, $\tau_f=301.5$ ppm/ $^{\circ}C$ with $x=0.03$ sintered at $1050^{\circ}C$. The variation of the permittivity is mainly determined by the volume fraction of the second phase and the relative density, while grain size and the phase composition are closely responsible for the change of $Q \times f$ values. Temperature coefficient move towards to a lower value, corresponding to the decline of ϵ_r .

Acknowledgements

This work is partly supported by the Science and Technology Planning Project of Guangdong Province, China (No.2017A010103001) and National Natural Science Foundation of China 51872037.

References

- [1] O'Bryan H M, Thomson J 2010 *J Am Ceram Soc* **57** 522
- [2] Dell'agli G, Spiridigliozzi L, Marocco A, Accardo G, Frattini D, Kwon Y, Yoon S P 2017 *Ceram Int* **43** 12799
- [3] Accardo G, Frattini D, Ham H C, Han J H, Yoon S P 2018 *Ceram Int* **44** 3800
- [4] Huang C L, Yang W R, Yu P C 2014 *J Eur Ceram Soc* **34** 277
- [5] Baumgarte A, Blachnik R 1992 *Mater Res Bull* **27** 1287
- [6] Kim D, Kim D, Hong K S 2000 *J Mater Res* **15** 1331
- [7] Park H S, Yoon K H, Kim E S 2010 *J Am Ceram Soc* **84** 99
- [8] Liao Q, Li L 2012 *Dalton Trans* **41** 6963
- [9] Liao Q, Li L, Zhang P, Cao L, Han Y 2011 *Solid State Sci* **13** 1201
- [10] Liao Q, Li L, Ding X, Ren X, Kabos P 2012 *J Am Ceram Soc* **95** 1501
- [11] Huan Z, Sun Q, Ma W, Wang L, Xiao F, Chen T 2013 *J Alloys Compd* **551** 630
- [12] Liao Q, Li L, Zhang P, Cao L, Han Y 2011 *Mater Sci Eng, B* **176** 41
- [13] Kim E S, Kang D H 2008 *Ceram Int* **34** 883
- [14] Li L, Cai H, Yu X, Liao Q, Gao Z 2014 *J Alloys Compd* **584** 315
- [15] Li L, Cai H, Ren Q, Sun H, Gao Z 2014 *Ceram Int* **40** 12213
- [16] Yang H, Li E, Duan S, He H, Zhang S 2017 *Mater Chem Phys* **199** 43
- [17] Li E, Yang H, Yang H, Zhang S 2018 *Ceram Int* **44** 8072
- [18] Li E, Yang Y, Yang H, Yuan Y, Zhang S 2018 *J Mater Sci: Mater Electron* **29** 11901
- [19] Yang H, Zhang S, Yang H, Zhang X, Li E 2018 *Inorganic chemistry* **57** 8264
- [20] Liu B, Huang Y H, Song K X, Li L, Chen X M 2018 *J Eur Ceram Soc* **38** 3833
- [21] Yang C F, Tzou W C, Chung H H, Diao C C, Huang C J 2009 *J Alloys Compd* **477** 673
- [22] Xiang M C, Yi L 2010 *J Am Ceram Soc* **85** 579
- [23] Li L, Liao Q, Zhang P 2009 *Ferroelectr* **388** 54
- [24] Huanping W, Qilong Z, Hui Y, Jiali Z 2004 *Electronic Components Materials* **23** 4
- [25] Mei Q J, Li C Y, Guo J D, Wu H T 2015 *J Alloys Compd* **626** 217